Approximate Expected Hypervolume Improvement for Parallel Expensive Multi-objective Optimization

1st Haihui Li
College of Computer Science
Sichuan University
Chengdu, China
haihui@stu.scu.edu.cn

2nd Zhenan He*
College of Computer Science
Sichuan University
Chengdu, China
zhenan@scu.edu.cn

3rd Suling Duan
School of Statistics
Chengdu University of Information Technology
Chengdu, China
dsl@cuit.edu.cn

***Abstract*—Many real-world optimization problems in science and engineering involve multiple conflicting objectives, with objective functions lacking explicit analytical form and computationally expensive to evaluate, which can be formulated as an expensive multi-objective optimization problem (EMOP). To address the challenge, multi-objective Bayesian optimization (MOBO) approaches approximating the Pareto front by using acquisition functions to select informative evaluation points, among which Expected Hypervolume Improvement (EHVI) is widely recognized for its ability to balance convergence and diversity. However, EHVI becomes computationally intractable for batch selection, requiring jointly evaluating improvements over multiple candidate solutions, and thus severely limits its scalability. To overcome this limitation, this paper introduces a decomposition-based approximate EHVI acquisition function that reformulates the original EHVI computation into a series of independent subproblems, each associated with a partial hypervolume improvement. This representation facilitates a novel batch selection strategy that jointly optimizes hypervolume improvement and sample diversity, promoting effective exploration of the Pareto front. In addition, a bi-level model management strategy is proposed to adaptively identify promising candidates and update surrogate models during the optimization process. Comprehensive experiments on synthetic and real-world benchmarks demonstrate that the proposed method achieves faster convergence and better diversity compared to several state-of-the-art MOBO algorithms.**

***Index Terms*—Multi-objective optimization, Bayesian optimization, Expected Hypervolume Improvement, Batch selection.**

I. Introduction

Multi-objective optimization problems (MOPs) are ubiquitous in real-world applications where multiple conflicting objectives must be optimized simultaneously to obtain a set of Pareto-optimal trade-off solutions [1]. However, in many practical settings, these objective functions lack explicit analytical form and are computationally expensive to evaluate. Typical examples include materials design [2], biological sequence design [3], and drug design [4], all of which naturally give rise to expensive multi-objective optimization problem (EMOP). Evolutionary algorithms, such as NSGA-II [5], MOEA/D [6], and SPEA2 [7], have shown remarkable success in solving standard MOPs by leveraging population-based search to approximate diverse Pareto fronts. Nevertheless, their reliance on a large number of objective evaluations combined with the lack of explicit problem formulations makes these algorithms impractical for EMOPs. This limitation underscores the need for more sample-efficient optimization frameworks that can preserve both convergence and diversity under stringent evaluation budgets.

To address the challenge of expensive objective evaluations, Bayesian Optimization (BO) [8] has emerged as a powerful and sample-efficient surrogate-based optimization paradigm. BO alleviates the computational burden by constructing probabilistic surrogate models to approximate the underlying objectives using a limited number of evaluations. An acquisition function is then employed to guide the selection of new evaluation points, balancing the exploration of uncertain regions with the exploitation of promising areas. Through this adaptive learning mechanism, BO can rapidly identify high-quality solutions with far fewer evaluations than traditional evolutionary algorithms.

Building upon these advantages, recent research has extended BO to multi-objective scenarios, giving rise to multi-objective Bayesian optimization (MOBO) methods capable of efficiently approximating Pareto fronts in expensive optimization settings. A common strategy is to integrate BO with evolutionary algorithms, either by employing surrogate models to approximate the expensive objectives and conducting an evolutionary search on the surrogates, or by explicitly optimizing acquisition functions to guide the selection of informative evaluation points [8].

In many MOBO frameworks, evolutionary search and surrogate modeling are tightly intertwined. For example, K-RVEA [9] employs surrogate models to predict objective values and adaptively selects real evaluation points by balancing prediction uncertainty and convergence pressure. Other methods place greater emphasis on the explicit optimization of BO-derived acquisition functions. ParEGO [10], for instance, randomly selects a reference vector in each iteration and transforms the multi-objective problem into a single-objective one using an augmented Tchebycheff scalarization; the next evaluation point is then obtained by maximizing the Expected Improvement (EI) of the scalarized objective. Similarly, MOEA/D-EGO [11] builds independent surrogate models for each objective and optimizes the expected Tchebycheff improvement within each subproblem, while additionally em-

*Corresponding author.

ploying *k-means* clustering to select multiple well-distributed candidates for real evaluation. These examples illustrate how representative MOBO methods implement surrogate-assisted evolution or acquisition-driven search in practice.

In MOBO, acquisition functions are critical, as they govern the selection of candidate solutions for actual evaluation. The EI acquisition function, which quantifies the anticipated utility of evaluating a candidate based on the surrogate model, is the cornerstone of BO [12]. Building on its proven effectiveness in single-objective optimization, researchers have extended the EI acquisition function to multi-objective settings by integrating it with multi-objective performance indicators. A prominent example is the Expected Hypervolume Improvement (EHVI) [13], which combines EI with the hypervolume indicator. In this framework, EHVI evaluates each candidate solution based not only on its contribution to enlarging the hypervolume of the current Pareto front (exploitation), but also uncertainty of the surrogate model (exploration). By maximizing EHVI at each iteration, the algorithm systematically selects evaluation points that are expected to advance convergence toward the Pareto front and maintain a diverse set of solutions, providing a principled and effective criterion for MOBO.

Despite these advancement, substantial challenges remain in scaling MOBO to real-world applications, especially when multiple real evaluations need to be executed in parallel [8], which is essential to reduce wall-clock time in expensive optimization scenarios. However, most existing EHVI-based algorithms are inherently sequential and therefore unable to leverage modern parallel computing infrastructures that can evaluate multiple solutions simultaneously. Although Monte Carlo-based extensions of EHVI have been proposed for batch evaluation [14], they require a large number of Monte Carlo samples to obtain a stable approximated value, resulting in computationally inefficient acquisition calculations and potentially unreliable decision making in practice.

To overcome these challenges, this work proposes a multi-objective Bayesian optimization algorithm based on approximate expected hypervolume improvement (AEHVIEGO) for expensive optimization problems. In AEHVIEGO, a surrogate-assisted search constructs an approximated Pareto front, which is then used to adaptively define informative reference points guiding EHVI computations along multiple search directions. Building on this, a decomposition-based approximated EHVI acquisition function reformulates the original EHVI into a set of tractable subproblems, each associated with a local hypervolume improvement component. By solving these subproblems collectively, a set of promising and well-distributed candidate solutions is generated, enabling efficient parallel batch evaluation. This is in clear contrast to classical EHVI, which tends to concentrate evaluations around a single optimum. In addition, a bi-level model management strategy is employed to select multiple highly promising solutions from this candidate set for real evaluation, ensuring efficient use of the limited evaluation budget. Together, these components enable AEHVIEGO to scale EHVI-based MOBO to parallel evaluation in computationally expensive real-world settings.

The main contributions of this paper are summarized as follows:

- An adaptive reference point selection mechanism is designed, which leverages the approximated Pareto front predicted by surrogate models to dynamically determine reference points, thereby providing more informative guidance for the EHVI computation.
- A decomposition-based approximate EHVI acquisition function is proposed, which reformulates EHVI into a set of tractable local subproblems and generates a well-distributed candidate set that naturally supports batch sampling.
- A bi-level model management strategy is introduced to select the most promising candidate solutions from this candidate set, ensuring efficient use of computational resources.

The remainder of this paper is organized as follows. Section II presents the necessary preliminaries. Section III provides a detailed description of the proposed AEHVIEGO. In Section IV, a series of numerical experiments are conducted to evaluate the performance of the proposed algorithm. Finally, Section V offers conclusions and discusses future directions.

II. Preliminaries

A. Gaussian Process

As a widely used surrogate model in BO, the Gaussian process (GP) [15], also known as the Kriging model, provides a probabilistic approximation of expensive objective functions. A key advantage of GP is that it offers both a predictive mean and an explicit measure of uncertainty. For any candidate solution $\mathbf{x}$, the response is modeled as

$$p(y \mid \mathbf{x}) \sim \mathcal{N}\big(\mu(\mathbf{x}),\, \sigma^2(\mathbf{x})\big) \tag{1}$$

where $\mu(\mathbf{x})$ and $\sigma(\mathbf{x})$ denote the predictive mean and standard deviation, respectively.

Given the observed data $\mathbb{D} = \{(\mathbf{x}_i, \mathbf{y}_i)\}_{i=1}^{N}$, the predictive mean and variance of GP at a test point $\mathbf{x}$ are given by

$$\mu(\mathbf{x}) = \mathbf{k}(\mathbf{x})^\top \mathbf{K}^{-1}\mathbf{y} \tag{2}$$

$$\sigma^2(\mathbf{x}) = k(\mathbf{x},\mathbf{x}) - \mathbf{k}(\mathbf{x})^\top \mathbf{K}^{-1}\mathbf{k}(\mathbf{x}) \tag{3}$$

where $k(\cdot,\cdot)$ is the kernel function of the GP, $\mathbf{k}(\mathbf{x}) = [k(\mathbf{x},\mathbf{x}_1),\ldots,k(\mathbf{x},\mathbf{x}_N)]^\top$ and $\mathbf{K}$ is the kernel matrix that contains the pairwise covariances between all training samples.

B. Expected Improvement

Among various acquisition functions, the EI is one of the most widely used due to its simplicity and effectiveness [12]. For a minimization problem with the current best value $\hat{y} = \min_{i=1,\ldots,N} \mathbf{y}_i$, EI measures the expected gain obtained by evaluating a candidate solution, favoring regions with low predictive mean and high uncertainty. Its closed-form expression is:

$$\mathrm{EI}(\mathbf{x}) = \big(\hat{y}-\mu(\mathbf{x})\big)\Phi\left(\frac{\hat{y}-\mu(\mathbf{x})}{\sigma(\mathbf{x})}\right)+\sigma(\mathbf{x})\phi\left(\frac{\hat{y}-\mu(\mathbf{x})}{\sigma(\mathbf{x})}\right) \tag{4}$$

where $\Phi(\cdot)$ and $\phi(\cdot)$ represent the cumulative distribution function and the probability density function of the standard normal distribution.

To extend EI to multi-objective optimization, EHVI was introduced. Given the current Pareto approximation $\hat{\mathcal{P}}$, the hypervolume improvement (HVI) contributed by a new objective vector $\mathbf{y}$ is

$$\mathrm{HVI}(\mathbf{y}, \hat{\mathcal{P}}) = \mathrm{HV}(\mathbf{y} \cup \hat{\mathcal{P}}) - \mathrm{HV}(\hat{\mathcal{P}}) \tag{5}$$

EHVI computes the expectation of HVI under the predictive distribution of the surrogate model:

$$\mathrm{EHVI}(\mathbf{x}) = \int_{\mathbb{R}^M} \mathrm{HVI}(\mathbf{y}, \hat{\mathcal{P}}) \prod_{m=1}^{M} \frac{1}{\sigma_m(\mathbf{x})} \phi\left(\frac{y_m - \mu_m(\mathbf{x})}{\sigma_m(\mathbf{x})}\right) \mathrm{d}y_m \tag{6}$$

Thus, EHVI generalizes EI by directly linking the acquisition function to the expected increase in the dominated hypervolume. However, its analytical evaluation quickly becomes intractable as the number of objectives grows, limiting its scalability in practice [16].

C. Hypervolume Approximation

Computing the exact hypervolume is prohibitive in high-dimensional objective spaces. To reduce this cost, several works propose approximation schemes based on the *Achievement Scalarizing Function* (ASF) [17]–[19]. The main idea is to estimate the HV by evaluating ASF values along multiple direction vectors, thereby transforming the original high-dimensional computation into a series of tractable one-dimensional aggregations.

Given a set of direction vectors $\mathbf{W}$ and a reference point $\mathbf{r}$, the ASF of a point $\mathbf{y}$ along $\mathbf{w} \in \mathbf{W}$ is defined as

$$\mathrm{ASF}(\mathbf{y} \mid \mathbf{w}, \mathbf{r}) = \min_{m \in \{1,\ldots,M\}} \left\{ \frac{r_m - y_m}{w_m} \right\} \tag{7}$$

The HV of a Pareto approximation $\hat{\mathcal{P}}$ can then be approximated by averaging the maximal ASF values along all sampled directions:

$$\mathrm{HV}(\hat{\mathcal{P}}, \mathbf{W}, \mathbf{r}) \approx \frac{1}{|\mathbf{W}|} \sum_{\mathbf{w} \in \mathbf{W}} \max_{\mathbf{y} \in \hat{\mathcal{P}}} \mathrm{ASF}(\mathbf{y} \mid \mathbf{w}, \mathbf{r}) \tag{8}$$

where $|\mathbf{W}|$ denotes the number of direction vectors.

As illustrated in Fig. 1, each direction vector emanates from the reference point $\mathbf{r}$ and intersects the Pareto front at a boundary point. The corresponding ASF value reflects the distance from $\mathbf{r}$ to the front along that direction, and averaging over multiple directions yields a computationally efficient approximation of the true HV.

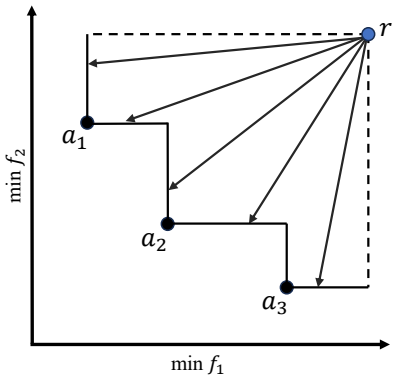

Fig. 1. Illustration of hypervolume approximation via ASF. Each direction vector from the reference point intersects the Pareto front at a boundary point.

III. Proposed Algorithm

A. The General Framework

The overall procedure of the proposed AEHVIEGO is summarized in **Algorithm 1**. The algorithm begins by generating NI initial samples in the decision space using Latin Hypercube Sampling (LHS) [20], a widely adopted design strategy for expensive optimization problems. This initialization improves the distributional coverage of the search space, enabling a more reliable surrogate construction in subsequent stages. All initial samples are then evaluated using the true objective functions and stored in the archive $\mathbb{A}$.

After initialization, the algorithm iteratively proceeds. At each iteration, independent GP models are constructed for each objective using archived data $\mathbb{A}$. Subsequently, a surrogate-assisted search is performed and the resulting population is used to approximate the Pareto front. This approximation then serves to determine the reference point for the current iteration. Guided by this reference point, the acquisition function is optimized across multiple search directions to identify a set of candidate solutions that balance the predicted improvement and uncertainty. Finally, the most promising candidate solutions from the optimized population are selected for real evaluation using the proposed bi-level model management strategy and incorporated into the archive. This iterative process continues until the maximum number of function evaluations is reached.

B. Surrogate-assisted Search

The purpose of this subsection is to use a surrogate-assisted evolutionary search to approximate the Pareto front and to dynamically determine the reference point for EHVI. In many existing EHVI-based methods, this point is obtained by first normalizing the objective values using either the current non-dominated set or the full archive of evaluated solutions and then adopting a fixed vector such as $\mathbf{r} = (1.1, \ldots, 1.1)^\top$ in the normalized M-dimensional objective space [21]. As illustrated in Fig. 2(a), ND-based normalization relies only on the evaluated non-dominated solutions (black points). Although this is simple, it tends to bias the search toward already explored regions: when these non-dominated points cover only a small portion of the true Pareto front, the resulting bounds restrict the hypervolume-improvement region, which severely limits exploration. Archive-based normalization, shown in Fig. 2(b), alleviates this locality issue by including all evaluated points, i.e., both non-dominated (black points) and dominated (yellow points) solutions. However, dominated solutions far from the Pareto front can drastically enlarge the normalized objective

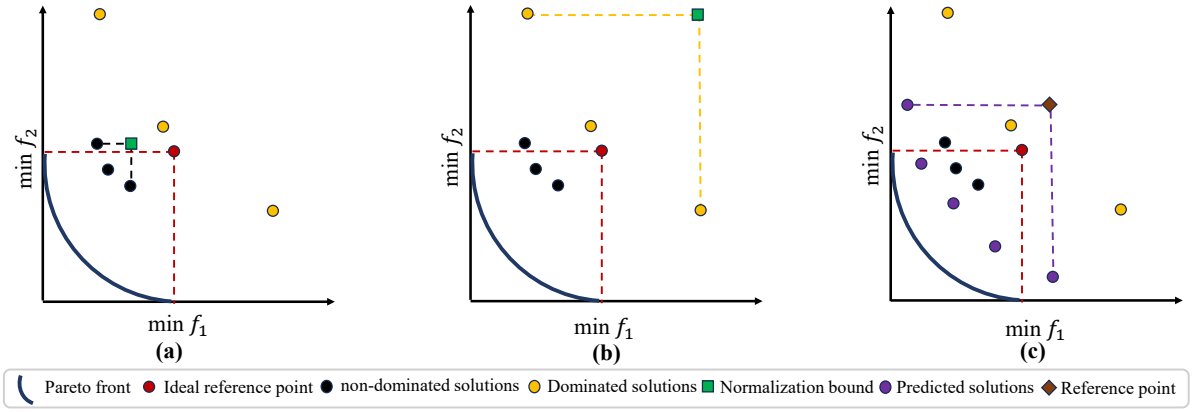

Fig. 2. Different strategies for reference point selection: **(a)** Normalization using evaluated non-dominated solutions, which may bias the search toward already explored regions. **(b)** Normalization using all evaluated solutions, where dominated points far from the front can distort the hypervolume search region. **(c)** The proposed surrogate-assisted strategy, which constructs an approximate Pareto front and adapts the reference point accordingly.

Algorithm 1: The Proposed AEHVIEGO Algorithm

Input: $\mathbf{F}$: expensive multi-objective functions; NI: the number of initial samples; N: the number of reference vectors; B: batch size; FE_{max}: the number of evaluation budget
Output: $\mathbb{A}$: Set of all evaluated points

Initialize NI samples using LHS
$\mathbb{A} \leftarrow$ Evaluate these initial samples using $\mathbf{F}$
$FE \leftarrow NI$
$\mathbf{W} \leftarrow$ Generate N reference vectors
while $FE < FE_{max}$ **do**
  Build GP models for each objective using $\mathbb{A}$;
  Perform surrogate-assisted search and determine the reference point $\mathbf{r}$;
  Optimize the acquisition function to obtain candidate solutions $\mathbf{X}$;
  Select B solutions from $\mathbf{X}$ for re-evaluation and add them to $\mathbb{A}$;
  $FE \leftarrow FE + B$;
return $\mathbb{A}$;

space and distort the effective search region, weakening the selection pressure required for convergence and diversity. Consequently, both strategies risk impairing the effectiveness of hypervolume-driven optimization.

To alleviate these limitations, we propose to determine the reference point from a surrogate-based approximation of the Pareto front, as illustrated in Fig. 2(c). Instead of relying directly on the evaluated solutions, a surrogate-assisted evolutionary search is first performed to construct an approximated Pareto front (purple points) predicted by the surrogate models, which captures the expected shape and extent of the true front beyond the positions of the sampled points (black and yellow). Rather than normalizing the entire archive, the reference point is then directly chosen as the Nadir point of this surrogate-based front, making it explicitly front-aware and less sensitive to outliers. thereby providing more reliable guidance for the EHVI computation.

To construct this approximate Pareto front, AEHVIEGO performs a surrogate-assisted evolutionary search guided by the GP models, as summarized in **Algorithm 2**. The archive $\mathbb{A}$ is used as the initial population. The offspring are then generated via crossover and mutation operators, and their objective values are predicted by the surrogate models. The parent and offspring populations are merged into a hybrid population, which is subsequently ranked by non-dominated sorting to provide the basis for environmental selection. For environmental selection, the algorithm follows the strategy of VaEA [22]. When the number of non-dominated solutions in the hybrid population exceeds the population size, the algorithm first preserves M extreme solutions and M best-converged solutions (i.e., those with the smallest Euclidean distance to the origin), ensuring that the extreme points are well captured and the approximate front remains representative. The remaining individuals are then selected according to cosine similarity and the Euclidean distance criterion to maintain diversity within the population.

Algorithm 2: SA-VaEA ($\mathbb{A}, \mathcal{M}$)

Input : Database $\mathbb{A}$; Surrogate models $\mathcal{M}$
Output: Approximate Pareto population $\mathbb{P}$

$t \leftarrow 1$;
$\mathbb{P} \leftarrow \mathbb{A}$;
while $t < T_{max}$ **do**
  $\mathbb{O} \leftarrow$ Generate offspring from $\mathbb{P}$ via crossover and mutation;
  $\mathbb{P} \leftarrow \mathbb{P} \cup \mathbb{O}$;
  Evaluate $\mathbb{P}$ using surrogate models $\mathcal{M}$;
  $\mathbb{P} \leftarrow$ Environmental selection of VaEA($\mathbb{P}$);
  $t \leftarrow t + 1$;

C. Optimization of the Acquisition Functions

In this step, we construct at each iteration a candidate population with high potential for subsequent expensive evaluation. To this end, the acquisition function is designed to approximate the EHVI, and its optimization should favor solutions that are expected to expand the hypervolume as much as possible, while balancing exploitation of the current Pareto front approximation and exploration of regions where the surrogate models remain uncertain. Therefore, this step focuses on constructing a tractable approximation of EHVI and developing an efficient procedure to optimize the resulting acquisition function.

The proposed method exploits geometric interpretation in [17], where the hypervolume is viewed as the average distance between the reference point and the Pareto front attainment surface, measured along multiple reference directions via the ASF. As illustrated in Fig. 3, when a candidate solution moves closer to the Pareto front, its ASF value relative to the reference point increases in one or more directions, thus contributing to the expansion of the hypervolume. The ASF improvements in two representative directions, $\mathbf{w}_1$ and $\mathbf{w}_2$, relative to the reference point $\mathbf{r}$, denoted by $\mathrm{I}_{\mathrm{ASF}}(\mathbf{y} \mid \mathbf{w}_1, \mathbf{r})$ and $\mathrm{I}_{\mathrm{ASF}}(\mathbf{y} \mid \mathbf{w}_2, \mathbf{r})$, quantify the contribution of a candidate solution $\mathbf{y}$ along these directions.

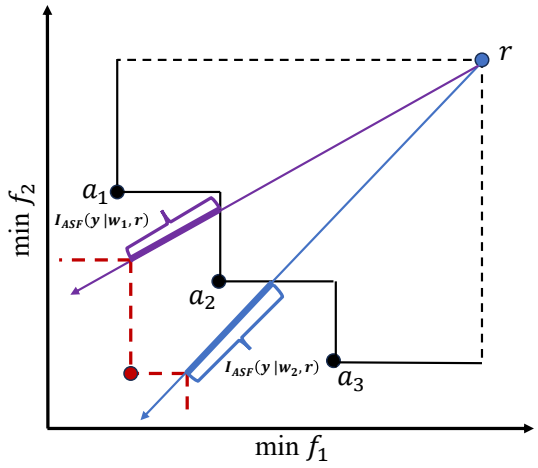

Fig. 3. Illustration of ASF improvement for a candidate solution (red point) in different reference direction.

For a given direction $\mathbf{w}$, the ASF is defined as in (7), and maximizing it is equivalent to minimizing $\max_{m=1,\ldots,M}\{(\mathbf{y_m} - \mathbf{r_m})/\mathbf{w_m}\}$. In the proposed framework, an independent GP model is constructed for each objective. Consequently, each affine transformation $(\mathbf{y_m} - \mathbf{r_m})/\mathbf{w_m}$ is Gaussian, and the ASF in the direction $\mathbf{w}$ becomes the maximum of several correlated Gaussian random variables. Although the exact distribution of this maximum is non-Gaussian, it can be well approximated using the MMA method [23], which yields a Gaussian approximation for the ASF scalar value in direction $\mathbf{w}$ at the design point $\mathbf{x}$.

Let $b_{\mathbf{w}}$ denote the best ASF value observed so far in direction $\mathbf{w}$. Since the scalarized ASF in each direction approximately follows a Gaussian distribution, the expected ASF improvement in direction $\mathbf{w}$ can be computed using the standard EI formula, which produces $\mathrm{EI}_{\mathrm{ASF}}(\mathbf{x} \mid \mathbf{w}, \mathbf{r})$. On this basis, the EHVI is approximated by the average expected ASF improvement over all reference directions. Let $\mathbf{W}$ denote the set of reference directions generated by the decomposition strategy, the approximate EHVI at the solution $\mathbf{x}$ is given by

$$\begin{aligned}\mathrm{AEHVI}(\mathbf{x}) &= \mathbb{E}_{\mathbf{y}\sim p(\mathbf{y}|\mathbf{x},\mathbb{D})}\left[\frac{1}{|\mathbf{W}|}\sum_{\mathbf{w}\in\mathbf{W}}\mathrm{I}_{\mathrm{ASF}}(\mathbf{y} \mid \mathbf{w}, \mathbf{r})\right] \\ &= \frac{1}{|\mathbf{W}|}\sum_{\mathbf{w}\in\mathbf{W}}\mathrm{EI}_{\mathrm{ASF}}(\mathbf{x} \mid \mathbf{w}, \mathbf{r})\end{aligned} \tag{9}$$

Once AEHVI is defined, the remaining task in this step is to efficiently optimize this acquisition function and thereby identify promising candidate solutions. To this end, the MOEA/D-GR algorithm [24] is adopted as the optimizer, where each reference direction is treated as a scalar subproblem associated with $\mathrm{EI}_{\mathrm{ASF}}$. The overall procedure for optimizing the AEHVI-based acquisition function is summarized in **Algorithm 3**. The optimization starts from an initial solutions $\mathbf{X}$ provided by the surrogate-assisted search, and the incumbent ASF value in each direction is calculated from the evaluated solutions $\mathbb{A}$ as the baseline $b_{\mathbf{w}}$. In each generation, MOEA/D-GR employs differential evolution and neighborhood-based replacement to update $\mathbf{X}$, and offspring solutions are assigned to the subproblem on which they achieve the largest $\mathrm{EI}_{\mathrm{ASF}}$. As optimization progresses, the population gradually concentrates on points with high expected ASF improvements, yielding a set of candidates that are both informative for surrogate refinement and effective for hypervolume expansion.

D. Bi-Level Model Management Strategy

After optimizing the acquisition function, a set of candidate solutions is obtained by maximizing $\mathrm{EI}_{\mathrm{ASF}}$ along multiple reference directions. This set contains solutions that appear promising under the surrogate predictions or exhibit substantial predictive uncertainty, thereby contributing both convergence potential and exploratory value.

Since only a limited number of expensive evaluations can be performed in EMOP, it becomes essential to determine which candidates should be selected for real evaluation. An ideal evaluation point should not only improve convergence and diversity in the objective space but also consider the prediction uncertainty of the surrogate model [25]. In other words, the infill criterion must maintain a well-balanced trade-off between exploitation and exploration.

To identify the most promising candidates for evaluation, we introduce a *bi-Level Model Management Strategy*, whose complete procedure is shown in **Algorithm 4**. The lower level focuses on convergence by selecting candidates with better predicted mean objective values from the surrogate-predicted population. The upper level then allocates the evaluation budget by maximizing the cumulative $\mathrm{EI}_{\mathrm{ASF}}$ across all reference

Algorithm 3: Acquisition Function Optimization

Input : $\mathbb{A}$: evaluated solutions; $\mathbf{X}$: initial solutions; $\mathbf{W}$: reference directions; $\mathbf{r}$: reference point; $\mathcal{M}$: surrogate models; δ: probability of selecting parents from the neighborhood; T: neighborhood size; G: number of generations;
Output: $\mathbf{X}$: a set of candidate solutions

$\mathrm{ASF}_{\min} \leftarrow$ compute minimum ASF value in each direction using $\mathbb{A}$
$\mathrm{EI}_{\mathrm{ASF}} \leftarrow$ calculate expected ASF improvement of $\mathbf{X}$ for all $\mathbf{w} \in \mathbf{W}$
for $g \leftarrow 1$ **to** G **do**
  for $i \leftarrow 1$ **to** N **do**
    $r \leftarrow$ generate a random number in $(0, 1)$
    if $r < \delta$ **then**
      $\boldsymbol{p} \leftarrow$ randomly select two parents from the neighborhood of $\mathbf{X}(i)$
    else
      $\boldsymbol{p} \leftarrow$ randomly select two parents from the entire population
    $\boldsymbol{o} \leftarrow$ generate offspring from $\mathbf{X}(i)$ and $\boldsymbol{p}$ via differential evolution
    $\mathrm{EI}_{\mathrm{ASF}}(\boldsymbol{o}) \leftarrow$ evaluate expected ASF improvement of $\boldsymbol{o}$ for all $\mathbf{w} \in \mathbf{W}$
    $j \leftarrow$ index of the subproblem with the maximum $\mathrm{EI}_{\mathrm{ASF}}(\boldsymbol{o})$
    update the neighborhood of subproblem j if $\mathrm{EI}_{\mathrm{ASF}}(\boldsymbol{o})$ exceeds that of the incumbent solution
return $\mathbf{X}$

directions. The overall selection problem can be formulated as follows:

$$\begin{aligned} \max_{\mathbf{X}^* \subseteq \mathbf{X^{nd}}} \quad & \frac{1}{|\mathbf{W}|} \sum_{\mathbf{w} \in \mathbf{W}} \max_{\mathbf{x} \in \mathbf{X}^*} \mathrm{EI}_{\mathrm{ASF}}(\mathbf{x} \mid \mathbf{w}, \mathbf{r}) \\ \text{s.t.} \quad & \mathbf{X^{nd}} = \min\left\{\mu_1(\mathbf{x}), \mu_2(\mathbf{x}), \ldots, \mu_M(\mathbf{x})\right\} \end{aligned} \tag{10}$$

where $\mu_1(\mathbf{x}), \mu_2(\mathbf{x}), \ldots, \mu_M(\mathbf{x})$ denote the posterior mean functions of the M objectives.

In the lower-level stage, the surrogate-predicted population is first ranked by non-dominated sorting and accumulated front by front until a candidate set $\mathbf{X}^{nd}$ is formed that approximates the current Pareto front. The upper-level stage then sequentially selects a batch of B solutions by maximizing the aggregated $\mathrm{EI}_{\mathrm{ASF}}$. After each selection, the solution $\mathbf{x}^*$ that maximizes the averaged expected improvement is added to $\mathbf{S}$ and removed from $\mathbf{X}^{nd}$. After each selection, the contribution of $\mathbf{x}^*$ is discounted in the improvement values of the remaining candidates. As selection progresses, the resulting batch $\mathbf{S}$ approximates the maximizer of the total expected improvement, providing a set of evaluation points that are both informative for surrogate refinement and effective for hypervolume expansion.

Algorithm 4: Bi-Level Model Management Strategy

Input : $\mathbf{X}$: Candidate population
B: Number of solutions to be re-evaluated
Output: $\mathbf{S}$: Selected promising solutions

$\mathbf{S} \leftarrow \emptyset$
`/* Lower-level process*/`
$\mathbf{X^{nd}} \leftarrow Nondominated\_sort(\mathbf{X})$
`/* Upper-level process*/`
Calculate $\mathrm{EI}_{\mathrm{ASF}}(\mathbf{x} \mid \mathbf{w}, \mathbf{r})$ for each $\mathbf{x} \in \mathbf{X^{nd}}$ and $\mathbf{w} \in \mathbf{W}$
for $i \leftarrow 1$ **to** B **do**
  $\mathbf{x}^* \leftarrow \arg\max_{\mathbf{x} \in \mathbf{X^{nd}}} \frac{1}{|\mathbf{W}|} \sum_{\mathbf{w} \in \mathbf{W}} \mathrm{EI}_{\mathrm{ASF}}(\mathbf{x} \mid \boldsymbol{w}, \boldsymbol{r})$
  $\mathbf{S} \leftarrow \mathbf{S} \cup \{\mathbf{x}^*\}$
  $\mathbf{X^{nd}} \leftarrow \mathbf{X^{nd}} \setminus \{\mathbf{x}^*\}$
  Update $\mathrm{EI}_{\mathrm{ASF}}$ of remaining solutions by subtracting the contribution of $\mathbf{x}^*$
return $\mathbf{S}$

IV. Empirical Studies

In this section, we evaluate the proposed algorithm on the ZDT [26] and DTLZ [27] benchmark suites. The number of decision variables is set to eight for the ZDT problems and to six for the DTLZ problems. Each algorithm is independently executed 20 times per benchmark, and the Wilcoxon rank-sum test with a significance level of 0.05 is used for statistical comparison. All experiments are implemented on the PlatEMO platform [28] and run on a laptop with an Intel Core i7 2.3 GHz CPU and 16 GB RAM.

A. Parameter Settings

The main parameter settings are summarized as follows. The number of initial samples is set to $11d-1$, where d denotes the number of decision variables. The maximum number of real function evaluations is 200 for bi-objective problems and 300 for problems with more than two objectives. The batch size for parallel evaluation is fixed to $B = 5$ in all experiments. GP models are built using the MATLAB DACE toolbox [29].

For reference vector generation, 200 vectors are generated via the simplex-lattice design for bi-objective problems, and the Uniform Normalized Vector method is used for higher-dimensional cases [30]. The population size is set equal to the number of reference vectors. The surrogate-assisted search runs for 20 iterations, and the acquisition function is optimized for 50 iterations per cycle. The parameters of MOEA/D-GR follow their default settings in the original implementation.

B. Performance Metrics

To assess both convergence and diversity, we adopt the Hypervolume (HV) and Inverted Generational Distance Plus (IGD^+) indicators [31].

TABLE I

STATISTICAL RESULTS OF THE IGD$^+$ VALUES ON THE ZDT AND DTLZ TEST PROBLEMS. THE SYMBOLS "+", "−", AND "≈" INDICATE SIGNIFICANTLY BETTER, WORSE, OR SIMILAR PERFORMANCE TO AEHVIEGO, RESPECTIVELY. BEST RESULTS ARE HIGHLIGHTED.

Problem	M	KRVEA	ABParEGO	PEIM	MOEADEGO	DirHVEGO	AEHVIEGO
ZDT1	2	1.7526e-2 (1.44e-3) −	7.6726e-2 (1.01e-1) −	5.2915e-2 (1.45e-2) −	2.3450e-2 (5.97e-3) −	4.3407e-3 (5.09e-4) −	2.8161e-3 (3.78e-4)
ZDT2	2	3.5189e-2 (3.23e-2) −	2.8011e-2 (8.03e-3) −	1.0156e-1 (1.83e-2) −	3.5068e-2 (1.45e-2) −	2.8716e-3 (1.15e-4) −	2.3128e-3 (6.99e-5)
ZDT3	2	1.6062e-2 (3.86e-3) −	8.7611e-2 (9.60e-2) −	5.2369e-2 (2.56e-2) −	2.7924e-1 (1.30e-1) −	3.6532e-2 (1.06e-1) −	3.8022e-3 (4.55e-3)
ZDT4	2	3.3317e+1 (1.21e+1) ≈	5.1749e+1 (8.74e+0) −	4.0739e+1 (1.23e+1) ≈	5.5419e+1 (8.17e+0) −	4.7679e+1 (1.14e+1) −	3.4496e+1 (9.35e+0)
ZDT6	2	1.1760e+0 (7.39e-1) −	3.9939e-1 (4.28e-1) ≈	2.8774e-1 (6.49e-2) ≈	1.0729e+0 (8.83e-1) −	2.0750e-1 (1.10e-1) ≈	2.7177e-1 (1.12e-1)
DTLZ1	2	2.7147e+1 (9.99e+0) ≈	3.7456e+1 (1.17e+1) ≈	4.5151e+1 (6.94e+0) −	4.9816e+1 (1.26e+1) −	5.4383e+1 (1.87e+1) −	3.1635e+1 (1.58e+1)
	3	2.3425e+1 (6.06e+0) ≈	2.4760e+1 (5.58e+0) −	2.2796e+1 (5.90e+0) ≈	2.6410e+1 (6.90e+0) −	1.6339e+1 (6.91e+0) ≈	1.8745e+1 (9.24e+0)
DTLZ2	2	1.2669e-2 (1.87e-3) −	3.0893e-2 (9.38e-3) −	1.8024e-2 (1.60e-3) −	7.8139e-2 (1.48e-2) −	4.5791e-3 (3.32e-4) −	1.9417e-3 (1.16e-4)
	3	3.3341e-2 (4.83e-3) −	9.6422e-2 (1.09e-2) −	3.0989e-2 (1.32e-3) −	1.0385e-1 (9.23e-3) −	2.3098e-2 (7.81e-4) +	2.3714e-2 (1.01e-3)
DTLZ3	2	5.8725e+1 (2.41e+1) ≈	8.1810e+1 (2.70e+1) ≈	9.3746e+1 (2.38e+1) −	1.0478e+2 (2.77e+1) −	1.0774e+2 (3.50e+1) −	7.0400e+1 (3.88e+1)
	3	5.7482e+1 (1.89e+1) −	6.6392e+1 (1.26e+1) −	5.7696e+1 (1.35e+1) −	6.0104e+1 (1.71e+1) −	4.5451e+1 (2.15e+1) ≈	3.8112e+1 (2.01e+1)
DTLZ4	2	2.3821e-1 (1.24e-1) −	1.1178e-1 (8.87e-2) ≈	1.8416e-1 (7.84e-2) −	1.8390e-1 (1.08e-1) ≈	1.5897e-1 (1.22e-1) ≈	1.2212e-1 (8.67e-2)
	3	1.3094e-1 (4.41e-2) +	2.5870e-1 (1.11e-1) ≈	2.1638e-1 (5.87e-2) ≈	2.1674e-1 (4.18e-2) ≈	2.3815e-1 (7.38e-2) ≈	2.3091e-1 (8.19e-2)
DTLZ5	2	1.2862e-2 (1.25e-3) −	3.5083e-2 (1.25e-2) −	1.8120e-2 (2.46e-3) −	7.7163e-2 (2.45e-2) −	4.6415e-3 (2.82e-4) −	1.9721e-3 (1.15e-4)
	3	1.8854e-2 (3.01e-3) −	2.8083e-2 (6.84e-3) −	8.3976e-3 (6.22e-4) −	5.8685e-2 (1.14e-2) −	5.4319e-3 (3.01e-4) −	2.8419e-3 (2.51e-4)
DTLZ6	2	1.4238e+0 (5.20e-1) −	6.1814e-1 (4.88e-1) −	8.1080e-2 (9.50e-3) +	8.1537e-1 (4.18e-1) −	4.7185e-2 (4.21e-2) +	8.4207e-2 (7.37e-2)
	3	8.6125e-1 (1.73e-1) −	3.6701e-1 (4.19e-1) −	3.7277e-2 (1.42e-2) ≈	3.3013e-1 (3.03e-1) −	4.7913e-2 (1.69e-2) ≈	4.4959e-2 (1.84e-2)
DTLZ7	2	1.3583e-2 (1.07e-3) −	2.7022e-2 (6.06e-3) −	3.6742e-2 (9.44e-3) −	2.1001e-2 (7.94e-3) −	6.1860e-3 (2.21e-3) −	1.8085e-3 (8.71e-5)
	3	5.5911e-2 (5.19e-3) +	9.0362e-2 (2.31e-2) +	2.2770e-2 (1.02e-3) +	6.6215e-2 (9.83e-3) +	4.6437e-2 (2.46e-2) +	3.1040e-1 (3.60e-1)
$+/-/\approx$		2/14/4	1/13/6	2/12/6	1/17/2	3/10/7	

1) HV*:* The HV metric measures the volume of the objective space dominated by the approximated Pareto front $\mathcal{P}$ with respect to a reference point $\mathbf{r}$:

$$\mathrm{HV}(\mathcal{P}) = \mathrm{Volume}\left(\bigcup_{\mathbf{y}\in\mathcal{P}} [\mathbf{y}_1, \mathbf{r}_1] \times \cdots \times [\mathbf{y}_m, \mathbf{r}_m]\right) \quad (11)$$

2) IGD$^+$*:* IGD$^+$ is an improved variant of IGD that simultaneously reflects convergence and diversity. It measures the average distance from each point in a reference set $\mathcal{P}^*$ (here 10,000 uniformly sampled points from the true Pareto front) to the closest point in the approximated Pareto front $\mathcal{P}$:

$$\mathrm{IGD}^+(\mathcal{P}, \mathcal{P}^*) = \frac{1}{|\mathcal{P}^*|} \sum_{\mathbf{p}\in\mathcal{P}^*} dis(\mathbf{p}, \mathcal{P}) \quad (12)$$

where $dis(\mathbf{p}, \mathcal{P})$ denotes the minimum Euclidean distance between $\mathbf{p}$ and to any point in the set $\mathcal{P}$. Smaller IGD$^+$ values indicate better performance.

C. Comparison with Other Algorithms

The comparative performance of AEHVIEGO and five state-of-the-art MOBO algorithms, namely KRVEA [9], ABParEGO [32], MOEA/D-EGO [11], PEIM [33] and DirHVEGO [34], is evaluated using the final IGD$^+$ values and convergence trajectories under identical evaluation budgets. The quantitative results reported in Table I demonstrate that AEHVIEGO delivers consistently strong performance across a broad set of ZDT and DTLZ benchmark problems. In the bi-objective ZDT problems (ZDT1–ZDT3) and the two-objective instances of DTLZ2, DTLZ5, and DTLZ7, AEHVIEGO attains the lowest IGD$^+$ values among all compared algorithms, indicating a closer approximation to the true Pareto front. This advantage carries over to the tri-objective benchmarks, where AEHVIEGO either outperforms or matches the best-performing algorithms across DTLZ1–DTLZ3, DTLZ5 and DTLZ6. The improvements are particularly pronounced on DTLZ3, a deceptive problem on which most algorithms exhibit notable performance degradation. Across the test suite, alternative methods generally show higher mean IGD$^+$ values and larger variances, indicating reduced robustness and less reliable performance under tight evaluation budgets.

The convergence behaviors shown in Fig. 4 further substantiate these findings. The IGD$^+$ trajectories across 19 benchmark problems indicate that AEHVIEGO achieves more rapid early-stage convergence and maintains consistently strong performance throughout the optimization process. On most ZDT and DTLZ problems, AEHVIEGO rapidly reduces IGD$^+$ within the first 50–80 evaluations, while KRVEA and ABParEGO typically converge more slowly and remain substantially farther away from the true Pareto front. PEIM and MOEA/D-EGO exhibit occasional fast improvements but tend to plateau early, indicating insufficient exploration or suboptimal selection pressure. DirHVEGO performs competitively on several problems. However, on many test functions AEHVIEGO converges to smaller IGD$^+$ values, indicating a more accurate approximation of the Pareto front under the same evaluation budget.

D. Performance on Real-World Application

A welded beam design problem [35] is further employed to assess the performance of AEHVIEGO in a realistic engineering scenario. The problem is formulated as a tri-objective EMOP, where three objectives, namely structural cost, end deflection, and a constraint-violation measure, must be minimized simultaneously. As shown in Fig. 5, all algorithms operate under the same limited evaluation budget and

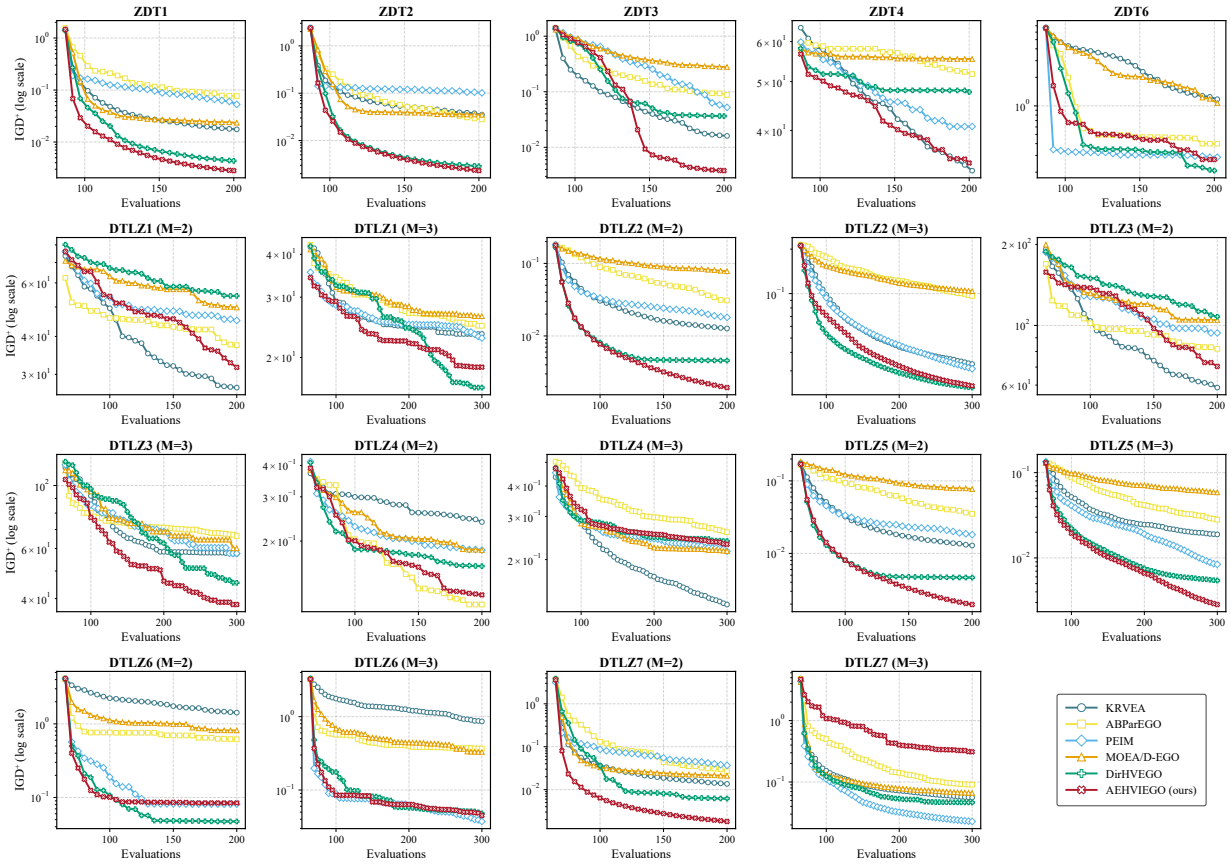

Fig. 4. IGD^+ convergence trajectories of the each algorithms across the ZDT and DTLZ benchmark suites, illustrating differences in optimization progress.

therefore obtain only a partial approximation of the true Pareto front. Nevertheless, AEHVIEGO achieves a markedly superior approximation quality, since it successfully identifies high-quality solutions on both sides of the Pareto-front knee, and thus captures the trade-off structure more comprehensively. In contrast, competing MOBO algorithms tend to converge toward only one side of the knee region, leading to narrower and more biased approximations. This observation is quantitatively supported by the final hypervolume values reported in Table II, where AEHVIEGO attains the largest HV among all compared methods, indicating better convergence and diversity on the welded beam problem.

V. Conclusion

This paper presented AEHVIEGO, a MOBO algorithm tailored for expensive optimization problems with parallel evaluations. By constructing a surrogate-assisted approximation of the Pareto front and adaptively selecting reference points, the proposed framework overcomes the limitations of conventional normalization-based strategies. In addition, a decomposition-based approximate EHVI formulation is employed to generate well-distributed candidate solutions that naturally support efficient parallel evaluation, while a bi-level model management mechanism selects promising solutions for real evaluation under strict budget constraints. Experimental results on the ZDT and DTLZ benchmark suites, as well as on a welded beam design problem, demonstrate that AEHVIEGO consistently outperforms several state-of-the-art MOBO algorithms in terms of overall optimization performance. Future work will focus on online adaptation of reference vector distributions during the optimization process to further enhance search guidance and improve performance on complex Pareto front geometries [36].

References

[1] A. Zhou, B.-Y. Qu, H. Li, S.-Z. Zhao, P. N. Suganthan, and Q. Zhang, "Multiobjective evolutionary algorithms: A survey of the state of the art," *Swarm and evolutionary computation*, vol. 1, no. 1, pp. 32–49, 2011.

[2] M. Ashby, "Multi-objective optimization in material design and selection," *Acta materialia*, vol. 48, no. 1, pp. 359–369, 2000.

[3] A. Taneda, "Multi-objective optimization for rna design with multiple target secondary structures," *BMC bioinformatics*, vol. 16, no. 1, p. 280, 2015.

[4] C. A. Nicolaou and N. Brown, "Multi-objective optimization methods in drug design," *Drug Discovery Today: Technologies*, vol. 10, no. 3, pp. e427–e435, 2013.

[5] K. Deb, A. Pratap, S. Agarwal, and T. Meyarivan, "A fast and elitist multiobjective genetic algorithm: Nsga-ii," *IEEE transactions on evolutionary computation*, vol. 6, no. 2, pp. 182–197, 2002.

[6] Q. Zhang and H. Li, "Moea/d: A multiobjective evolutionary algorithm based on decomposition," *IEEE Transactions on Evolutionary Computation*, vol. 11, no. 6, pp. 712–731, 2007.

[7] E. Zitzler, M. Laumanns, and L. Thiele, "Spea2: Improving the strength pareto evolutionary algorithm," *TIK report*, vol. 103, 2001.

TABLE II
STATISTICAL RESULTS OF THE HV VALUES ON THE WELDED BEAM DESIGN PROBLEM.

Problem	M	D	KRVEA	ABParEGO	PEIM	MOEA/D-EGO	DirHVEGO	AEHVIEGO
Welded Beam Design	3	4	9.8724e-1 (1.98e-2) −	9.9626e-1 (2.15e-3) −	9.9719e-1 (1.67e-3) −	9.9316e-1 (4.76e-3) −	9.9893e-1 (4.76e-4) −	9.9935e-1 (4.65e-5)
$+/-/\approx$			0/1/0	0/1/0	0/1/0	0/1/0	0/1/0	

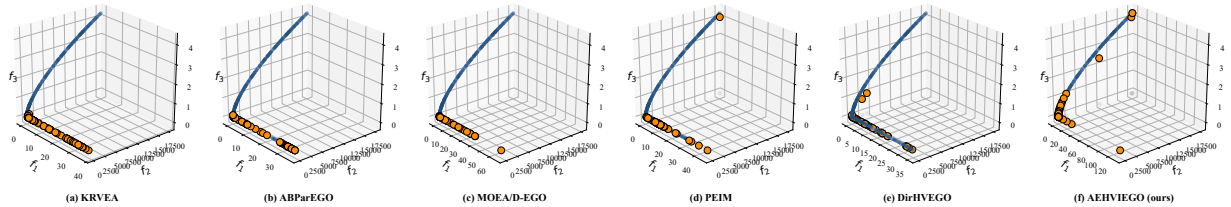

Fig. 5. Optimization results on the welded beam design problem. Blue points represent the true Pareto front, while orange markers denote the solutions obtained by the different algorithms.

[8] X. Wang, Y. Jin, S. Schmitt, and M. Olhofer, "Recent advances in bayesian optimization," *ACM Computing Surveys*, vol. 55, no. 13s, pp. 1–36, 2023.

[9] T. Chugh, Y. Jin, K. Miettinen, J. Hakanen, and K. Sindhya, "A surrogate-assisted reference vector guided evolutionary algorithm for computationally expensive many-objective optimization," *IEEE Transactions on Evolutionary Computation*, vol. 22, no. 1, pp. 129–142, 2016.

[10] J. Knowles, "Parego: A hybrid algorithm with on-line landscape approximation for expensive multiobjective optimization problems," *IEEE transactions on evolutionary computation*, vol. 10, no. 1, pp. 50–66, 2006.

[11] Q. Zhang, W. Liu, E. Tsang, and B. Virginas, "Expensive multiobjective optimization by moea/d with gaussian process model," *IEEE Transactions on Evolutionary Computation*, vol. 14, no. 3, pp. 456–474, 2009.

[12] D. R. Jones, M. Schonlau, and W. J. Welch, "Efficient global optimization of expensive black-box functions," *Journal of Global optimization*, vol. 13, pp. 455–492, 1998.

[13] M. T. Emmerich, K. C. Giannakoglou, and B. Naujoks, "Single-and multiobjective evolutionary optimization assisted by gaussian random field metamodels," *IEEE Transactions on Evolutionary Computation*, vol. 10, no. 4, pp. 421–439, 2006.

[14] S. Daulton, M. Balandat, and E. Bakshy, "Differentiable expected hypervolume improvement for parallel multi-objective bayesian optimization," *Advances in neural information processing systems*, vol. 33, pp. 9851–9864, 2020.

[15] C. K. Williams and C. E. Rasmussen, *Gaussian processes for machine learning*. MIT press Cambridge, MA, 2006, vol. 2, no. 3.

[16] L. Mei and Z. Dawei, "Pointwise expected hypervolume improvement for expensive multi-objective optimization," *Journal of Global Optimization*, vol. 91, no. 1, pp. 171–197, 2025.

[17] K. Shang, H. Ishibuchi, and X. Ni, "R2-based hypervolume contribution approximation," *IEEE Transactions on Evolutionary Computation*, vol. 24, no. 1, pp. 185–192, 2019.

[18] Y. Nan, K. Shang, and H. Ishibuchi, "What is a good direction vector set for the r2-based hypervolume contribution approximation," in *Proceedings of the 2020 Genetic and Evolutionary Computation Conference*, 2020, pp. 524–532.

[19] J. Deng and Q. Zhang, "Approximating hypervolume and hypervolume contributions using polar coordinate," *IEEE Transactions on Evolutionary Computation*, vol. 23, no. 5, pp. 913–918, 2019.

[20] M. D. McKay, R. J. Beckman, and W. J. Conover, "A comparison of three methods for selecting values of input variables in the analysis of output from a computer code," *Technometrics*, vol. 42, no. 1, pp. 55–61, 2000.

[21] B. Wang, H. K. Singh, and T. Ray, "Adjusting normalization bounds to improve hypervolume based search for expensive multi-objective optimization," *Complex & Intelligent Systems*, vol. 9, no. 2, pp. 1193–1209, 2023.

[22] Y. Xiang, Y. Zhou, M. Li, and Z. Chen, "A vector angle-based evolutionary algorithm for unconstrained many-objective optimization," *IEEE Transactions on Evolutionary Computation*, vol. 21, no. 1, pp. 131–152, 2016.

[23] C. E. Clark, "The greatest of a finite set of random variables," *Operations Research*, vol. 9, no. 2, pp. 145–162, 1961.

[24] Z. Wang, Q. Zhang, A. Zhou, M. Gong, and L. Jiao, "Adaptive replacement strategies for moea/d," *IEEE transactions on cybernetics*, vol. 46, no. 2, pp. 474–486, 2015.

[25] F. Li, Y. Yang, Y. Liu, Y. Liu, and M. Qian, "Bi-level model management strategy for solving expensive multi-objective optimization problems," *IEEE Transactions on Emerging Topics in Computational Intelligence*, 2024.

[26] K. Deb, "Multi-objective genetic algorithms: Problem difficulties and construction of test problems," *Evolutionary computation*, vol. 7, no. 3, pp. 205–230, 1999.

[27] K. Deb, L. Thiele, M. Laumanns, and E. Zitzler, "Scalable multi-objective optimization test problems," in *Proceedings of the 2002 congress on evolutionary computation. CEC'02 (Cat. No. 02TH8600)*, vol. 1. IEEE, 2002, pp. 825–830.

[28] Y. Tian, R. Cheng, X. Zhang, and Y. Jin, "Platemo: A matlab platform for evolutionary multi-objective optimization [educational forum]," *IEEE Computational Intelligence Magazine*, vol. 12, no. 4, pp. 73–87, 2017.

[29] S. N. Lophaven, H. B. Nielsen, J. Søndergaard *et al.*, *DACE: a Matlab kriging toolbox*. Citeseer, 2002, vol. 2.

[30] Y. Nan, K. Shang, and H. Ishibuchi, "What is a good direction vector set for the r2-based hypervolume contribution approximation," in *Proceedings of the 2020 Genetic and Evolutionary Computation Conference*, 2020, pp. 524–532.

[31] J. G. Falcón-Cardona and C. A. C. Coello, "Indicator-based multi-objective evolutionary algorithms: A comprehensive survey," *ACM Computing Surveys (CSUR)*, vol. 53, no. 2, pp. 1–35, 2020.

[32] X. Wang, Y. Jin, S. Schmitt, and M. Olhofer, "An adaptive bayesian approach to surrogate-assisted evolutionary multi-objective optimization," *Information Sciences*, vol. 519, pp. 317–331, 2020.

[33] D. Zhan, J. Qian, J. Liu, and Y. Cheng, "Pseudo expected improvement matrix criteria for parallel expensive multi-objective optimization," in *World Congress of Structural and Multidisciplinary Optimisation*. Springer, 2017, pp. 175–190.

[34] L. Zhao and Q. Zhang, "Hypervolume-guided decomposition for parallel expensive multiobjective optimization," *IEEE Transactions on Evolutionary Computation*, vol. 28, no. 2, pp. 432–444, 2023.

[35] T. Ray and K. Liew, "A swarm metaphor for multiobjective design optimization," *Engineering optimization*, vol. 34, no. 2, pp. 141–153, 2002.

[36] K. Shang, T. Shu, and H. Ishibuchi, "Learning to approximate: Auto direction vector set generation for hypervolume contribution approximation," *IEEE Transactions on Evolutionary Computation*, vol. 28, no. 1, pp. 105–116, 2022.